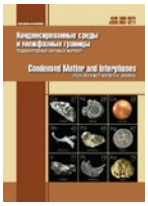

ISSN 1606-867X (Print)
ISSN 2687-0711 (Online)
Condensed Matter and Interphases
Kondensirovannye Sredy i Mezhfaznye Granitsy
https://journals.vsu.ru/kcmf/

Original articles

Research article
https://doi.org/10.17308/kcmf.2026.28/13968

Phase composition and molecular bonds of hybrid porous silicon nanostructures with precipitated cinnarizine

E. P. Domashevskaya[1]✉, A. S. Lenshin[1,2], Yu. A. Polkovnikova[1], O. V. Chernousova[2], V. E. Frolova[1], I. E. Zanin[1]

[1]*Voronezh State University,*
1, Universitetskaya pl., Voronezh 394018, Russian Federation

[2]*Voronezh State University of Engineering Technologies,*
19, Revolution av., Voronezh 394036, Russian Federation

Abstract

Objectives: This study aimed to form hybrid porous silicon – cinnarizine (CIN/por-Si) nanostructures and investigate their phase composition and molecular bonds.

Experimental: Cinnarizine was deposited on por-Si wafers using two methods: chemical deposition of cinnarizine in a hydrochloric acid solution and mechanical spin-coating of a cinnarizine-containing solution, both at room temperature and with heating to 50 °C. The resulting samples were analyzed using X-ray diffraction (XRD) analysis and optical IR and UV spectroscopy.

Conclusions: XRD results revealed the predominance of the amorphous cinnarizine phase in the CIN/por-Si hybrid nanostructures, with preservation of its molecular structure, as characterized by IR spectroscopy. UV spectroscopy revealed an additional direct band-to-band transition in the absorption spectra of the CIN/por-Si hybrid nanostructures, not belonging to por-Si, with an energy of ~1.5 eV. This transition may be related to the optical absorption properties of cinnarizine within the nanostructure, caused by its bonding with porous silicon.

Keywords: Mesoporous silicon (por-Si), Crystalline and amorphous cinnarizine (CIN), Hybrid CIN/por-Si nanostructures, IR transmission spectra, UV absorption spectra

Funding: This study was supported by grant No. 25-22-00292 from the Russian Science Foundation (RSF) and with financial support from the Ministry of Education and Science of the Russian Federation under the State Assignment for Universities in the Field of Scientific Activity, Project No. FZGU-2029-0006.

For citation: Domashevskaya E. P., Lenshin A. S., Polkovnikova Yu. A., Frolova V. E., Chernousova O. V., Zanin I. E. Phase composition and molecular bonds of hybrid nanostructures of porous silicon with precipitated cinnarizine. *Condensed Matter and Interphasis*. 2026;28(3): 396–407. https://doi.org/10.17308/kcmf.2026.28/13968

✉ Evelina P. Domashevskaya, e-mail: ftt@phys.vsu.ru
© Domashevskaya E. P., Lenshin A. S., Polkovnikova Yu. A., Frolova V. E., Chernousova O. V., Zanin I. E., 2026

The content is available under Creative Commons Attribution 4.0 License.

Оригинальные статьи

Научная статья
УДК 535
Научная специальность ВАК – 1.3.8. Физика конденсированного состояния;
1.3.21. – Медицинская физика
https://doi.org/10.17308/kcmf.2026.28/13968

Фазовый состав и молекулярные связи гибридных наноструктур пористого кремния с осажденным циннаризином

Э. П. Домашевская[1]✉, А. С. Леньшин[1,2], Ю. А. Полковникова[1], О. В. Черноусова[2], В. Е. Фролова[1], И. Е. Занин[1]

[1]ФГБОУ ВО «Воронежский государственный университет», Университетская пл., 1, Воронеж 394018, Российская Федерация

[2]ФГБОУ ВО "Воронежский государственный университет инженерных технологий», пр. Революции, 19, Воронеж 394036, Российская Федерация

Аннотация

Целью работы являлось формирование гибридных наноструктур пористый кремний – циннаризин CIN/por-Si и исследование особенностей их фазового состава и молекулярных связей.

Экспериментальная часть: Осаждение циннаризина на пластины кремния с por-Si производилось двумя способами: химическим методом осаждения циннаризина в растворе соляной кислоты и механическим методом spin-coating нанесения раствора с циннаризином как при комнатной температуре, так и с подогревом до 50 °C. Сформированные образцы исследовались методами рентгенофазового анализа (РФА) и оптической ИК- и УФ-спектроскопии.

Выводы: Результаты РФА исследований показали преобладание аморфной фазы циннаризина в гибридных наноструктурах CIN/por-Si с сохранением его молекулярной структуры, охарактеризованной данными ИК-спектроскопии. Методом УФ- спектроскопии в спектрах поглощения гибридных наноструктур CIN/por-Si обнаружен дополнительный прямой зона-зонный переход, не принадлежащий por-Si, с энергией ~ 1.5 эВ, природа которого может быть связана с особенностями оптического поглощения циннаризина в составе наноструктуры, обусловленными образованием его связей с пористым кремнием.

Ключевые слова: мезопористый кремний por-Si, кристаллический и аморфный циннаризин CIN, гибридные наноструктуры CIN/por-Si, ИК-спектры пропускания, УФ-спектры поглощения

Источник финансирования: Исследование выполнено за счет гранта Российского научного фонда РНФ № 25-22-00292 и при финансовой поддержке Минобрнауки РФ в рамках Госзадания для университетов в области научной деятельности, проект № ФЗГУ-2029-0006

Для цитирования: Домашевская Э. П., Леньшин А. С., Полковникова Ю. А., Фролова В. Е., Черноусова О. В., Занин И. Е. Фазовый состав и молекулярные связи гибридных наноструктур пористого кремния с осажденным циннаризином. *Конденсированные среды и межфазные границы*. 2026;28(3): 396–407. https://doi.org/10.17308/kcmf.2026.28/13968

✉ Домашевская Э. П., e-mail: ftt@phys.vsu.ru

© Домашевская Э. П., Леньшин А. С., Полковникова Ю. А., Фролова В. Е., Черноусова О. В., Занин И. Е., 2026

1. Introduction

Among the various drug carriers, porous silicon (por-Si) is of particular interest [1–3], with one area of current application being biomedicine. In biomedical devices, por-Si can be used as various functional elements [4–9]: as a carrier material for targeted drug delivery, including multiple drugs simultaneously; as photosensitizers in photodynamic therapy; in tissue engineering; in various types of biosensors; for biomedical imaging, including tumor visualization; and in the treatment of eye diseases.

Modified porous silicon layers can be used in biosensors for various purposes [10]. Biosensors and lab-on-a-chip devices based on por-Si are used to detect various analytes, including glucose, DNA, antibodies, viruses, and bacteria. These include electrical, electrochemical, optical, and tag-based sensors [11].

Porous silicon has attracted considerable attention as a drug delivery carrier due to its unique properties, such as biocompatibility, large pore size with uniform distribution, and large surface area [12, 13]. Experiments conducted both

in vitro and *in vivo* indicate minimal or no toxicity of porous silicon [14–17].

Various groups of drugs are currently used to treat cerebral diseases, including calcium channel blockers, one of which is the widely used and affordable drug cinnarizine [18–20].

Cinnarizine has a vasodilatory effect, improves cerebral and peripheral circulation, exhibits antihistamine activity, reduces vestibular excitability, and lowers sympathetic tone. Furthermore, cinnarizine, a white or pale yellow, odorless crystalline powder, is virtually insoluble in water, which may reduce its bioavailability when taken orally [22–26]. On the pharmaceutical market, the active pharmaceutical ingredient is available in single dosage form—tablets, making it promising to expand the range of cinnarizine dosage forms.

One of the mandatory studies of developed drugs is preclinical toxicological studies, particularly the assessment of the damaging effects of a drug candidate upon a single administration (acute toxicity) and repeated administration (chronic toxicity) [27]. Currently, toxicological studies using second-order biological models, in which protozoa are used as biological objects, are of particular importance [28]. Laboratory animals and cell cultures are often used as models. Preclinical studies are among the most economically justified as a rapid assessment of the toxicometric parameters of objects. Studies using second-order biological models do not have a negative impact from the standpoint of humanity and legality. In particular, it has been shown [29] that the Paramecium caudatum ciliate cell culture is an adequate test object for identifying the acute toxicity of substances and its use is possible in toxicological studies.

In our previous work [30], we developed a method for the adsorption-desorption of cinnarizine onto porous silicon and tested the use of Paramecium caudatum cell culture to determine the toxicity of por-Si nanopowders with and without cinnarizine precipitation. The optimal adsorption time for cinnarizine on the surface of por-Si mesoporous silicon (30 minutes) and the desorption time for cinnarizine from the por-Si surface (45 minutes) were determined. The increase in desorption time compared to adsorption time demonstrates the potential of using mesoporous silicon for the precipitation of cinnarizine and its subsequent delivery for therapeutic purposes.

In the same study [30], we demonstrated the feasibility of using Paramecium caudatum ciliate cell culture to study the toxicity of mesoporous silicon nanopowders and the same powders with precipitated cinnarizine. When studying the toxicity of porous silicon nanoparticles on the test object of the protozoan Paramecium caudatum, we found that mesoporous silicon nanopowders increased their viability in a functional load test without exhibiting toxic effects, while silicon nanopowders with precipitated cinnarizine could reduce the viability of the ciliates.

In the present study, we expanded the methods for applying cinnarizine to porous silicon and focused on the results of the interfacial interaction of cinnarizine with mesoporous silicon (por-Si).

This study aims to form hybrid cinnarizine-porous silicon (CIN/por-Si) nanostructures using two methods: chemical precipitation of cinnarizine in a hydrochloric acid solution and mechanical spin-coating of a cinnarizine solution onto por-Si. The study also investigates their phase composition and molecular bonding using X-ray diffraction (XRD) analysis and optical IR and UV spectroscopy.

2. Research objects and methods

In the experimental studies, 1-(Diphenylmethyl)-4-(3-phenyl-2-propenyl) piperazine (CAS No. 298-57-7) was used as the active pharmaceutical ingredient of cinnarizine (CIN). Its structural formula is shown in Fig. 1. The chemical formula of cinnarizine is $C_{26}H_{28}N_2$.

2.1. Preparation and studying methods of the samples on porous silicon

Porous silicon (por-Si) samples were obtained by double-sided anodic electrochemical etching of c-Si(100) single-crystal silicon wafers polished on both sides in alcohol solutions of hydrofluoric acid with the addition of hydrogen peroxide in constant current mode, followed by rinsing in distilled water and isopropyl alcohol. To obtain por-Si, n-type c-Si(100) wafers with a resistivity of 0.3 Ohm·cm were used.

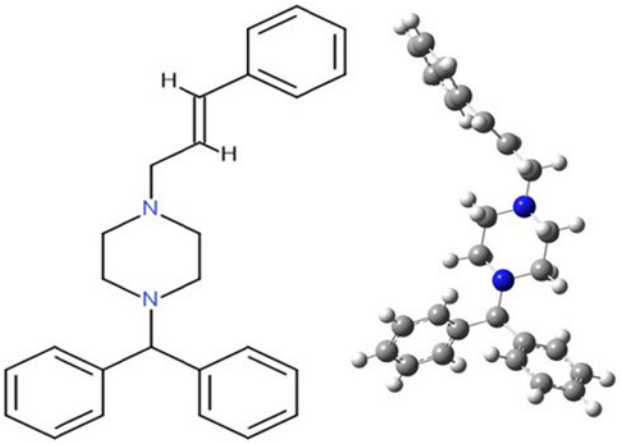

Fig. 1. Structural formula of cinnarizine 1–(Diphenylmethyl)–4–(3–phenyl–2–propenyl)piperazine (CIN)

The solution composition and electrochemical etching conditions for mesoporous silicon are described in detail in our studies [31–33]. At an etching rate of ~1 μm/min, the thickness of the mesoporous silicon por-Si layer was ~10 μm with an average pore diameter of 50–100 nm. The porosity of the samples, determined in our previous studies [31–33], was 50 %.

Fig. 2 shows images of a cleavage (left) and a surface (right) of one of the samples of mesoporous silicon por-S, obtained with a JSM–6380LV scanning electron microscope, JEOL of the Center for Collective Use of Scientific Equipment of Voronezh State University.

To study the features of the phase composition, microstructure, and molecular bonds in samples with different methods of depositing cinnarizine on wafers with mesoporous por-Si layers with a thickness of about 10 μm, four samples of CIN/por-Si nanostructures were prepared: sample 2 CIN/por-Si with chemically deposited cinnarizine, in which CIN deposition was carried out by keeping the sample in a 0.1 M aqueous solution of hydrochloric acid with the addition of cinnarizine for 30 minutes at room temperature; Sample 3 CIN/por-Si with chemically deposited cinnarizine (analogous to sample 2), but with the solution heated to 50 °C; sample 4 CIN/por-Si, in which the cinnarizine solution was deposited on por-Si using the spin-coating method on a Spin NXG setup for 1 minute at a rotation speed of 1000 rpm; sample 5 CIN/por-Si is analogous to sample 4, but with heating to 50 °C during sample rotation. Sample 1, the initial por-Si mesoporous silicon, and sample 6, the initial commercial cinnarizine CIN powder, were studied as comparison standards.

X-ray diffraction analysis of the obtained samples was performed in the Center for Collective Use of Scientific Equipment of Voronezh State University with PANalytical EMPYREAN diffractometer (The Netherlands) using Cu$K\alpha$ radiation and a PIXcel1D position-sensitive detector.

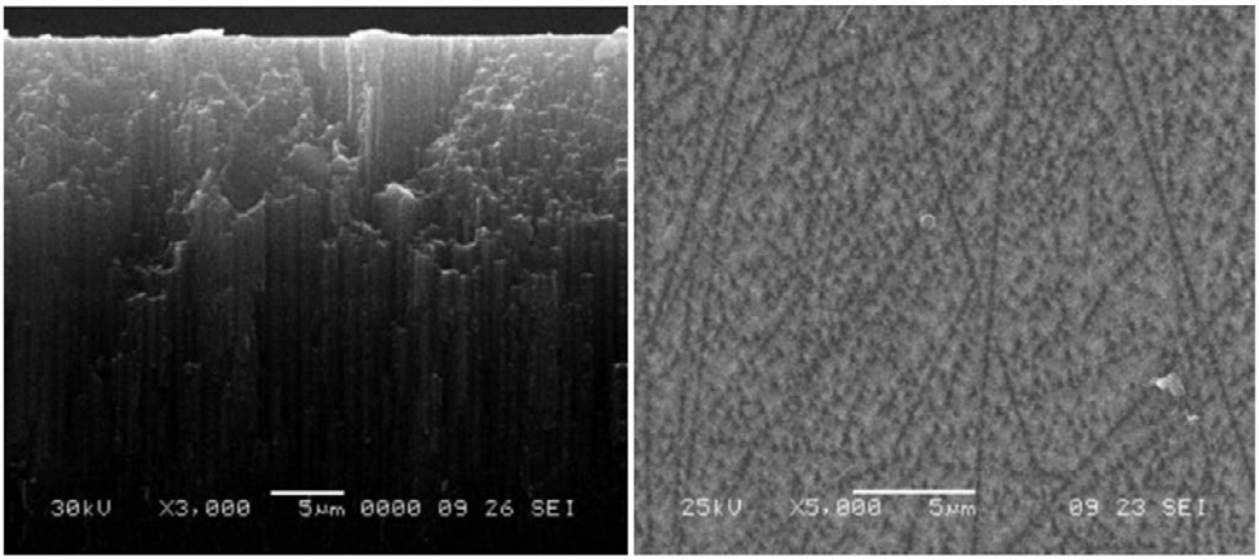

Fig. 2. SEM images of the cleavage (left) and surface (right) of a sample of mesoporous silicon por-Si obtained by electrochemical etching of a single-crystal silicon wafer c-Si(100)

Measurements were performed in reflection mode, with θ/2θ scanning in 0.02° increments along 2θ. The measurement range was 2θ = 8–80°. The diffractometer calibration was verified prior to the study using the external standard NIST-SRM676. Interplanar spacings and integrated intensities were calculated based on profile analysis (Pauli method) of experimental diffraction patterns using the HighScore Plus software suite, Version: 3.0.t (3.0.5), Date: 30-01-2012. Produced by: PANalytical B.V. Amelo, The Netherlands.

X-ray diffraction analysis was performed using the PDF-2 powder diffraction database of the International Center for Diffraction Data (ICDD).

The size of silicon nanocrystals in the porous por-Si layer was estimated using the Scherrer formula:

$$D = \frac{K\lambda}{\beta \cos\theta}, \quad (1)$$

where D is the crystallite size, K is a constant close to 0.9, λ is the wavelength $K\alpha 1$ of the characteristic radiation, β is the half-width of the X-ray line (hkl) used for the analysis, and θ is the Bragg angle for the plane (hkl).

The study of molecular bonds in the samples using IR spectroscopy was conducted in the Center for Collective Use of Scientific Equipment of Voronezh State University using Vertex Bruker 70 FT-IR spectrometer (Germany) with an absorption/transmission attachment. The positions of the IR spectral modes in the samples with precipitated cinnarizine were determined using the AIST database: Spectral Database for Organic Compounds (SDBS) [34].

Optical properties of the samples were obtained in the 190–900 nm range using UV spectroscopy on a Perkin Elmer LAMBDA 650 instrument. UV transmission-reflectance spectra were converted to absorption spectra to identify optical absorption features in por-Si and CIN/por-Si porous layers using Bruker's OPUS software and the Lambert–Bouguer formula:

$$T = \exp[-D], \quad (2)$$

where T is the transmittance and D is the optical density.

3. Results and discussion

3.1. XRD studies of samples obtained by different methods of cinnarizine deposition on por-Si/c-Si(100) wafers

For X-ray diffraction studies of the phase composition and microstructural features in samples with different methods of CIN cinnarizine deposition on mesoporous silicon por-Si, four hybrid CIN/por-Si samples were prepared. Their diffractograms are shown in Fig. 3 (samples No. 2–5), along with the diffraction patterns of por-Si mesoporous silicon (sample No. 1) and CIN cinnarizine powder (sample No. 6) as comparison standards.

Table 1 shows the values of the Bragg angles 2θ° of the diffraction lines, the interplanar distances d (Å) of the crystalline phases and the relative intensities of the I % reflection lines of all the samples studied shown in Fig. 3.

The corresponding X-ray structural data d (Å)/I % from the International Database ICDD with the numbers of the PDF-2 X-ray diffraction data maps are given in square brackets.

First of all, a careful comparison of the interplanar distances d_{hkl} and the relative intensities of the I % lines of the por-Si/c-Si(100) sample No. 1 with the ICDD tabular data showed the presence in the composition of sample No. 1 of not only crystalline silicon (lines Si(220) at 2θ = 47.7402° and Si(311) at 2θ = 56.3418° and the most intense line Si(400) at 2θ = 69.1457° from a single-crystal c-Si(100) plate with ten-micron layers of porous silicon), but also two different phases of silicon dioxide SiO_2: tetragonal syngony (line at 2θ = 33.0060°) and cubic syngony of zeolite (lines at 2θ = 61.7053° and 2θ = 66.6391°), which are also present in all samples No. 2–No. 5 with precipitated cinnarizine (see Fig. 3 and Table 1).

A visual comparison of the diffractograms of all the samples in Fig. 3 suggests that, when deposited on porous silicon, cinnarizine CIN transforms from the initial crystalline state of the monoclinic syngony [ICDD 00-043-1593] to an amorphous state, and in the diffraction patterns of the hybrid nanostructures of the CIN/por-Si samples (No. 2–No. 5), the lines from por-Si/c-Si(100) predominate, with only traces of the most intense lines from cinnarizine in samples CIN/por-Si No. 2 and CIN/por-Si No. 3.

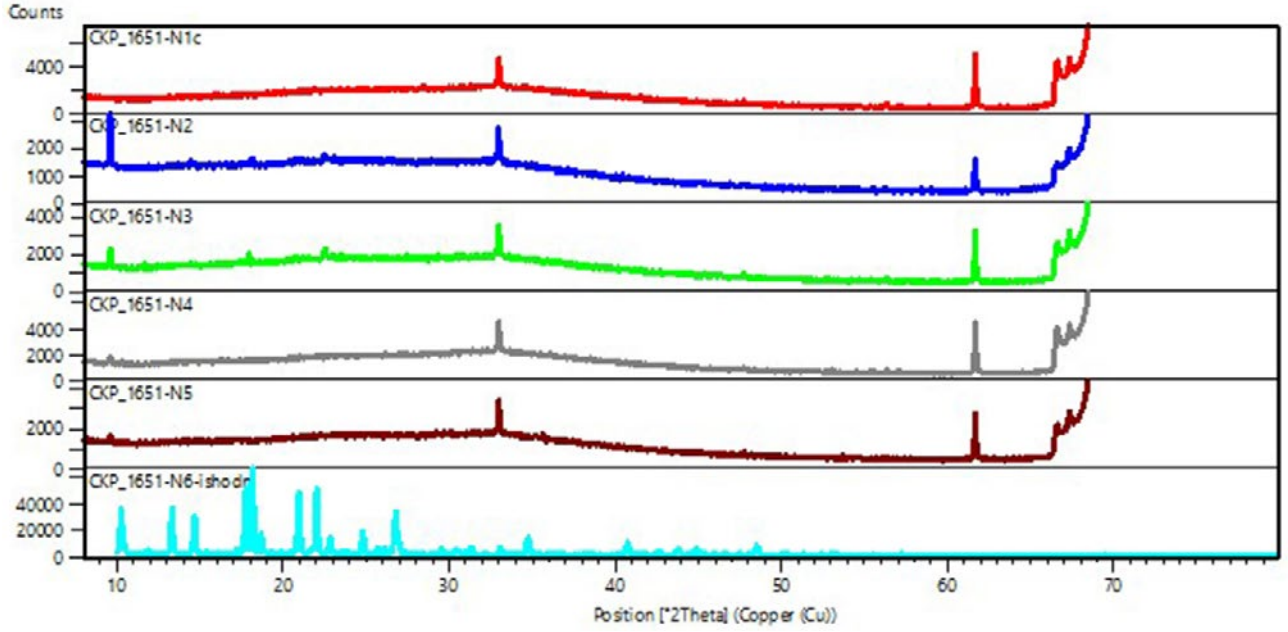

Fig. 3. Diffraction patterns of samples (top to bottom): *1* – initial por-Si/c-Si(100) (reference standard); sample *2* – CIN/por-Si: chemical deposition of cinnarizine on por-Si in 0.1 M aqueous hydrochloric acid solution for 30 minutes at room temperature; sample *3* – CIN/por-Si – analog of sample 2 with heating of the solution to 50 °C; sample *4* – CIN/por-Si: deposition of cinnarizine solution on por-Si by spin-coating for 1 minute and rotation speed of 1000 rpm; sample *5* – CIN/por-Si – analog of sample *4*, with heating to 50 °C during sample rotation; sample *6* – initial commercial cinnarizine powder CIN/ (reference standard)

However, a careful comparison of d_{hkl}/I % for all samples with the ICDD tabulated data indicates a more complex interaction between CIN and por-Si during the chemical deposition of cinnarizine on porous silicon using two different methods. During the chemical deposition of cinnarizine in an aqueous hydrochloric acid solution at room temperature and with heating to 50 °C, CIN/por-Si samples No.2 and No.3, along with an increase in the intensity of the background lines of the diffraction patterns from the amorphous phase of cinnarizine, show traces of three very weak reflections in the 2θ range of 11–23° originating from the most intense lines of monoclinic cinnarizine, indicating a small proportion of the crystalline phase as a result of its chemical deposition in por-Si, regardless of heating.

With another method of depositing cinnarizine solution on por-Si by the spin-coating method, in CIN/por-Si samples No. 4 and No. 5, not even traces of the crystalline phase in the deposited amorphous cinnarizine were observed in the corresponding diffraction patterns (see Fig. 3 and Table 1).

At the same time, in the diffraction patterns of all four samples, regardless of the deposition method, along with other SiO_2 phases (cubic and tetragonal), a new rhombohedral phase of silicon dioxide SiO_2 [ICDD 01-089-0735] appears in the form of the first intense line at 2θ = 9.6087° with values d = 9.205-9.195 Å and I = 34–11 %. It should be noted that the rhombohedral phase of SiO_2 did not appear on the original por-Si sample, unlike the cubic and tetragonal phases. Therefore, its appearance in all four hybrid CIN/por-Si samples may be the result of physicochemical interactions during the introduction of cinnarizine into por-Si, which itself is completely amorphized (samples No. 4 and No. 5) or with a small content of the crystalline phase (samples No. 2 and No. 3).

In connection with this experimental fact of our study, it is worth noting the result of work [38], which showed that cinnarizine precipitated during *in vitro* lipolysis in a self-emulsifying drug delivery system (SMEDDS) is not crystalline, suggesting either its amorphous form or molecular dispersion.

Table 1. Interplanar distances *d*(Å) and relative intensities *I* % of diffraction lines of CIN/por-Si hybrid nanostructure samples and of the original por-Si and CIN samples

2θ°	Por-Si No. 1 *d*(Å)/*I* %	No. 2 *d*(Å)/*I* %	No. 3 *d*(Å)/*I* %	No. 4 *d*(Å)/*I* %	No. 5 *d*(Å)/*I* %	No.6 CIN *d*(Å)/*I* %
9.6087 10.2493 [10.237]	– –	9.202/34 [9.174/100 **SiO_2 rhombo-hedral** ICDD 01-089-0735] –	9.202/34 [9.174/100 **SiO_2 rhombo-hedral** ICDD 01-089-0735] –	9.202/34 [9.174/100 **SiO_2 rhombo-hedral** ICDD 01-089-0735] –	9.202/34 [9.174/100 **SiO_2 rhombo-hedral** ICDD 01-089-0735] –	– 8.623/44 [8.634/35 CIN ICDD 00-043-1593]
11.839	–	7.557/9 – –	7.557/9 – –	– – –	– – –	7.470/4 [7.468/2] 6.650/45 [6.647/5] 6.038/38 [6.033/11]
18.1461	– – – – –	4.940/17 – – – –		– – – – –	– – – – –	4.992/68 [4.985/6] 4.885 /100 [4/877/31] 4.750/22 [4.742/100] 4.240/57 [4.237/35] 4.034/58 [4.028/13]
22.8866	– –	3.944/18 –	3.944/17 –	– –	– –	3.892/19 [3/884/11] 3.587/25 [3.583/18]
33.0060 [33.128]	2.714/0.13 [2.702/100 **SiO_2 tetra-gonal** ICDD 00-047-1300]	2.714/57	2.714/57]	2.714/54 [	2.714/65	2.702/33 [2.702/2]
47.7402 [47.304]	1.905/0.02 [1.920/55 **Si(220)** ICDD 00-027-1402]	1.905/9	1.904/8	1.906/3	1.905/8	
56.3418 [56.122]	1.633/0.02 [1.637/30 **Si(311)** ICDD 00-027-1402]	1.634/3	1.634/3	1.633/7	1.633/5	
61.7053 [61.677] 66.6391 [66.190] 67.3873 69.1457	1.503/0.26 1.403/0.23 [1.502/23 SiO_2 (046) и (137) 1.410/2.3 **SiO_2 cubic, zeolite** ICDD 98-017-0504] 1.390/0.25 1.357/100 [1.357/6 **Si(400)** ICDD 00-027-1402]	1.503/95 1.403/77 1.390/100 Si(400)	1.503/95 1.403/77 1.390/100 Si(400)	1.503/100 1.403/92 1.390/98 Si(400)	1.503/92 1.404/70 1.390/100 Si(400)	

To confirm the results of cinnarizine deposition on porous silicon with amorphization, we studied its intramolecular bonds using IR spectroscopy.

3.2. Study of molecular bonds of CIN/por-Si nanostructures using IR spectroscopy

IR spectroscopy is a universal method for obtaining information about the molecular structure of a substance [39] and allows us to determine the nature of atomic groups, the nature of chemical bonds, and their changes under external conditions. Each molecule has its own unique vibrational spectrum, so by comparing the obtained experimental spectrum with known literature data, the substance under study can be identified.

Fig. 4 shows the IR spectra of the same six samples presented in previous X-ray diffraction studies, including four hybrid CIN/por-Si samples (samples No. 2–No. 5), along with samples of mesoporous por-Si silicon (sample No. 1) and cinnarizine powder (sample No. 6) as reference standards.

The IR spectrum of the reference sample of mesoporous por-Si (sample No. 1) clearly shows bands characteristic of porous silicon Si-Si (616 cm^{-1}), Si-O-Si (460, 1060 cm^{-1}), Si-Hx (860 cm^{-1}) [32], which after the deposition of cinnarizine in por-Si become less pronounced or even disappear completely, as in sample No.3. This method, in turn, most fully preserves all intramolecular bonds of cinnarizine in the hybrid nanostructure of CIN/por-Si sample No. 3. Furthermore, visual inspection revealed the appearance of a translucent white film on all CIN/por-Si samples, corresponding to the color of the cinnarizine solution.

3.4. Optical studies of the CIN/por-Si nanostructure by UV spectroscopy

Optical studies in the visible and near-UV regions are a significant complement to X-ray diffraction analysis, as absorption spectra in this region provide information on the band gap, impurity levels, band-to-band transition types, and other parameters.

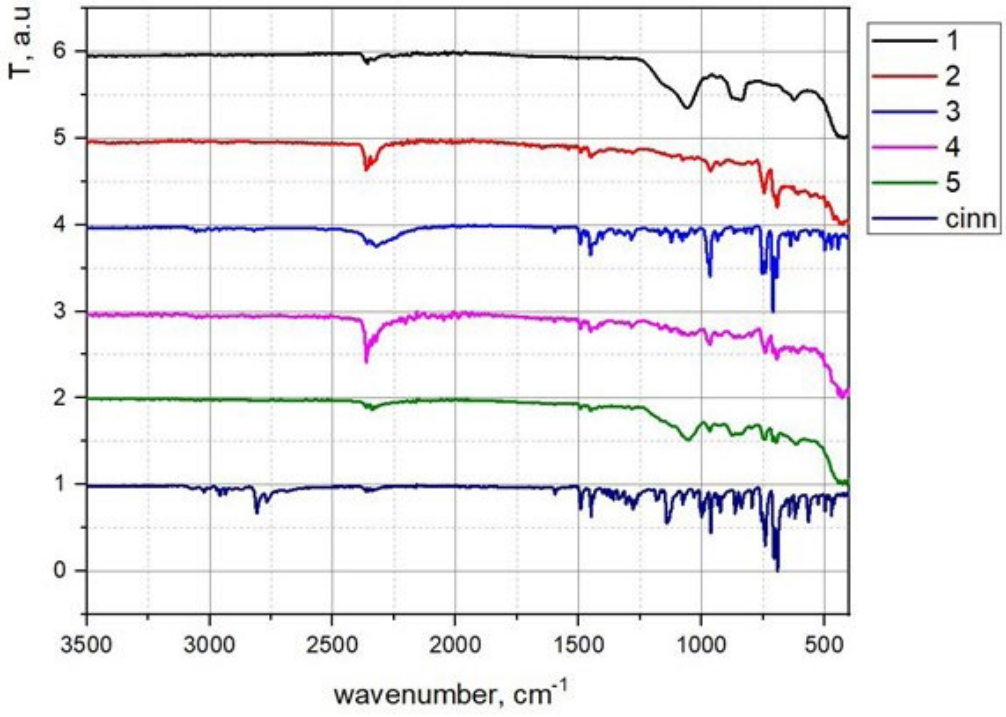

Fig. 4. IR transmission spectra of samples (top-bottom): *1* – original por-Si/c-Si(100) (reference standard); sample *2* – CIN/por-Si: chemical deposition of cinnarizine on por-Si in 0.1 M aqueous hydrochloric acid solution for 30 minutes at room temperature; sample *3* – CIN/por-Si – analog of sample *2* with heating of the solution to 50 °C; sample *4* – CIN/por-Si: deposition of cinnarizine solution on por-Si by spin-coating for 1 minute and rotation speed of 1000 rpm; sample *5* – CIN/por-Si – analog of sample *4*, with heating to 50 °C during sample rotation; sample *6* – original commercial cinnarizine powder CIN/ (reference standard)

Table 2. The presence of cinnarizine and porous silicon vibration modes in the IR transmission spectra of CIN/por-Si hybrid nanostructures obtained by using two methods of its deposition on the por-Si surface

Vibration modes (cm^{-1})		Samples					
Interatomic bonds		1(por-Si)	2	3	4	5	cinn
Si-O-Si rocking	480	+	+	+	+	+	
Si-Si stretching	616	+	+	+	+	+	
$SiH(SiO_2)$ bending O_3–SiH bending	830–880	+	+	+	+	+	
val. =CH	**962, 999**	–	+	+	+	+	+
Si-O-Si asymmetric stretching	1060-1200	–	–	+	+	+	
C-N val. stretch	**1134**	–	–	+	–	–	+
C–H, bend	**1350**	–	–	+	–	–	+
C=C, stretch	1462	–	+	+	+	+	+
valence C=C bonds in an aromatic ring	**1597**	–	–	+	–	–	+
CO_2	2350	+	+	+	+	+	+
C–H, stretch	**2850–3000**	–	–	–	–	–	+

Fig. 5 presents the UV absorption spectra in coordinates of the dependence of $(D{\cdot}h\nu)^2$ on the quantum energy for the por-Si sample (Fig. 5a), as well as for sample No. 2 (porous silicon with deposited cinnarizine CIN/por-Si) (Fig. 5b), which were calculated from the optical UV reflectance spectra using the Kramers-Kronig relations [40].

Graphical analysis allows us to identify individual sections with a linear dependence of $(D{\cdot}h\nu)^2$ on the quantum energy, which may indicate the presence of direct allowed band-to-band transitions in this spectral region. Linear extrapolation to the zero value of $(D{\cdot}h\nu)^2$ allows us to determine the energy of direct transitions characteristic of the samples. The intersection of tangent lines to the linear sections with the energy coordinate in Fig. 5a determines the values of possible direct transitions in por-Si with an energy of ~2.4 eV, corresponding according to [39] to mesoporous silicon nanocrystals with dimensions of ~2 nm, and with an energy of ~1.9 eV, corresponding to mesoporous silicon nanocrystals of ~3 nm.

In Fig. 5b, for CIN/por-Si sample No.2 with deposited cinnarizine, the same procedure reveals, in addition to the two transitions listed

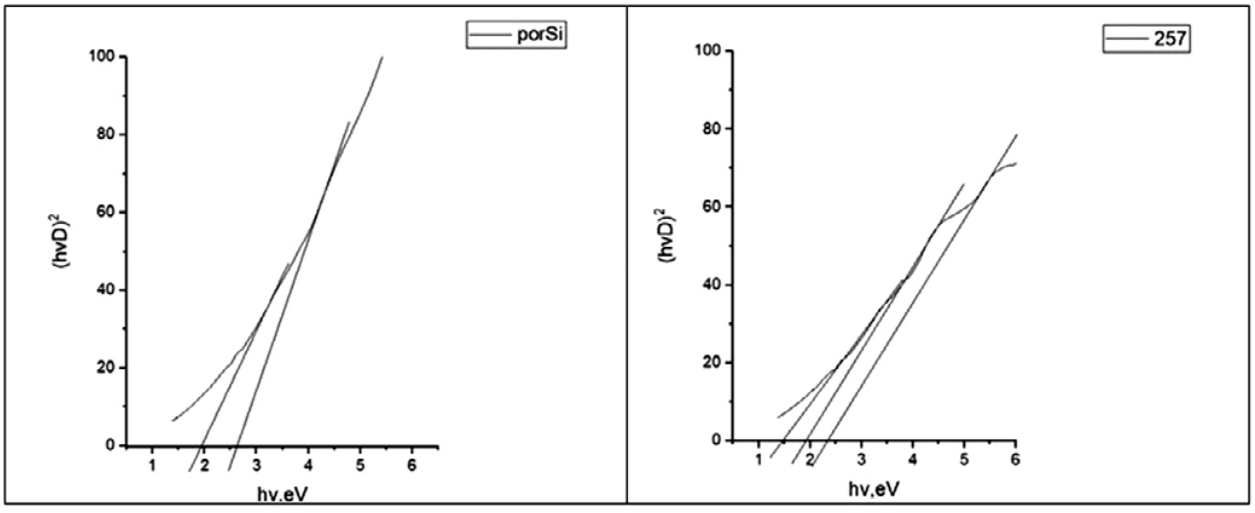

Fig. 5. UV absorption spectra in coordinates of the dependence of $(D{\cdot}h\nu)^2$ on the quantum energy for a) the initial porous silicon por-Si and b) porous silicon with deposited cinnarizine CIN/por-Si (sample No. 2)

above, an additional direct transition with an energy of ~1.5 eV, the nature of which may be related to the optical absorption characteristics of cinnarizine within the nanostructure, caused by the formation of bonds with porous silicon. Determining the mechanism for the occurrence of this direct transition in the CIN/por-Si hybrid nanostructure requires us to continue further thorough research in this area.

4. Conclusion

As a result of achieving the objectives of this study, samples of hybrid porous silicon-cinnarizine CIN/por-Si nanostructures were formed using two modified methods: chemical deposition of cinnarizine on por-Si in a hydrochloric acid solution and mechanical spin-coating of a cinnarizine solution on por-Si, both at room temperature and heated to 50 °C.

The resulting samples were studied using X-ray diffraction (XRD) analysis and optical IR and UV spectroscopy. Based on the analysis of the new results of CIN/por-Si hybrid nanostructures studies, the following conclusions can be drawn:

– As a result of physicochemical interactions during chemical deposition on por-Si, crystalline cinnarizine amorphizes with a small content of the crystalline phase or becomes completely amorphous using the mechanical spin-coating method of depositing a cinnarizine solution on por-Si.

– In all the studied samples of CIN/por-Si hybrid nanostructures, regardless of the method of cinnarizine deposition, a rhombohedral phase of SiO_2 was detected, which did not appear on the original por-Si sample, in contrast to the cubic and tetragonal phases of SiO_2, present in both por-Si and all CIN/por-Si samples.

– IR spectroscopy revealed the preservation of the main components of the molecular structure of both the deposited cinnarizine and the porous silicon matrix in CIN/por-Si hybrid nanostructures, regardless of the method of chemical deposition of cinnarizine. The molecular structure was most completely preserved with chemical deposition of cinnarizine, with heating to 50 °C during deposition.

– UV spectroscopy revealed an additional direct band-to-band transition in the absorption spectra of the CIN/por-Si hybrid nanostructure, not belonging to por-Si, with an energy of ~1.5 eV. This transition may be related to the optical absorption properties of cinnarizine within the nanostructure, caused by the formation of bonds with porous silicon.

Thus, the obtained results of the studies of CIN/por-Si hybrid nanostructures show that control of the condensed phase, amorphous or crystalline, as well as the molecular structure of deposited cinnarizine on porous silicon, may prove to be useful information in the development of its various dosage forms to increase the overall absorption of the drug.

Authors' contributions

Domashevskaya E. P. – methodology development, results description, writing and editing the text, final conclusions. Lenshin A. S. – method development, sample collection, results interpretation, text writing, final conclusions. Polkovnikova Yu. A. – toxicology studies and results description. Frolova V. E. – research implementation, results presentation. Chernousova O. V. – research implementation, results presentation. Zanin I. E. – X-ray phase analysis of the samples.

Conflict of interests

The authors declare that they have no known competing financial interests or personal relationships that could have influenced the work reported in this paper.

References

1. Santos H. A., Mäkilä E., Airaksinen A. J., Bimbo L. M., Hirvonen J. Porous silicon nanoparticles for nanomedicine: preparation and biomedical applications. *Nanomedicine*. 2014;9(4): 535–54. https://doi.org/10.2217/nnm.13.223

2. Eremina A. S., Kargina Y. V., Kharin A. Y., Timoshenko V. Y., Petukhov D. I. Mesoporous silicon nanoparticles covered with peg molecules by mechanical grinding in aqueous suspensions. *Microporous and Mesoporous Materials*. 2022;331: 111641. https://doi.org/10.1016/j.micromeso.2021.111641

3. Canham L. T. Bioactive silicon structure fabrication through nanoetching techniques. *Advanced Materials*. 1995;7(12): 1033–1037. https://doi.org/10.1002/adma.19950071215

4. Park J.-H., Gu L., von Maltzahn G., Ruoslahti E., Bhatia S. N.; Sailor M. J. Biodegradable luminescent porous silicon nanoparticles for in vivo applications. *Nature Materials*. 2009;8(4): 331–336. https://doi.org/10.1038/nmat2398

5.Qi S., Zhang P., Ma M., ... Zhang H. Cellular internalization–induced aggregation of porous silicon nanoparticles

for ultrasound imaging and protein-mediated protection of stem cells. *Small*. 2019;5(1): 1804332. https://doi.org/10.1002/smll.201804332

6.Yan J., Siwakoti P., Shaw S., Bose S., Kokil G., Kumeria T. Porous silicon and silica carriers for delivery of peptide therapeutics. *Drug Delivery and Translational Research*. 2024;14(12): 3549–3567. https://doi.org/10.1007/s13346-024-01609-7

7. Maximchik P. V., Tamarov K., Sheval E. V., ... Osminkina L. A. Biodegradable porous silicon nanocontainers as an effective drug carrier for regulation of the tumor cell death pathways. *ACS Biomaterials Science & Engineering*. 2019;5: 6063–6071. https://doi.org/10.1021/acsbiomaterials.9b01292

8. Wang F., Hui H., Barnes T. J., Barnett C., Prestidge C. A. Oxidized mesoporous silicon microparticles for improved oral delivery of poorly soluble drugs. *Molecular Pharmaceutics*. 2010;7: 227–236. https://doi.org/10.1021/mp900221e

9. Chew T. L., Ahmad A. L., Bhatia S. Ordered mesoporous silica (OMS) as an adsorbent and membrane for separation of carbon dioxide (CO_2). *Advances in Colloid and Interface Science*. 2010;153(1–2): 43–57. https://doi.org/10.1016/j.cis.2009.12.001

10. Li W., Liu Z., Fontana F., ... Santos H. A. Tailoring porous silicon for biomedical applications: from drug delivery to cancer immunotherapy. *Advanced Materials*. 2018;30: 1703740. https://doi.org/10.1002/adma.201703740

11. Peng F., Cao Z., Ji X., Chu B, Su Y., He Y. Silicon nanostructures for cancer diagnosis and therapy. *Nanomedicine (Lond)*. 2015;10: 2109–2123. https://doi.org/10.2217/nnm.15.53

12. Bakshi S., Pandey P., Mohammed Y., ... Kumeria T. Porous silicon embedded in a thermoresponsive hydrogel for intranasal delivery of lipophilic drugs to treat rhinosinusitis. *Journal of Controlled Release*. 2023;363: 452–463. https://doi.org/10.1016/j.jconrel.2023.09.045

13. Kilpelainen M., Riikonen J., Vlasova M. A., ... Jarvinen K. In vivo delivery of a peptide, ghrelin antagonist, with mesoporous silicon microparticles. *Journal of Controlled Release*. 2009;137: 166–170. https://doi.org/10.1016/j.jconrel.2009.03.017

14. Low S. P., Williams K. A., Canham L. T., Voelcker N. H. Evaluation of mammalian cell adhesion on surface-modified porous silicon. *Biomaterials*. 2006;27: 4538–4546. https://doi.org/10.1016/j.biomaterials.2006.04.015

15. Korhoen E., Rönkkö S., Hillebrand S., ... Kauppinen A. Cytotoxicity assessment of porous silicon microparticles for ocular drug delivery. *European Journal of Pharmaceutics and Biopharmaceutics*. 2016;100: 1–8. https://doi.org/10.1016/j.ejpb.2015.11.020

16. Mohammadpour R., Cheney D. L., Grunberger J. W., ... Ghandehari H. One-year chronic toxicity evaluation of single dose intravenously administered silica nanoparticles in mice and their ex vivo human hemocompatibility. *Journal of Controlled Release*. 2020;324: 471–481. https://doi.org/10.1016/j.jconrel.2020.05.027

17. Ferreira M. P., Ranjan S., Correia A. M., ... Santos H. A. In vitro and in vivo assessment of heart-homing porous silicon nanoparticles. *Biomaterials*. 2016;94: 93–104. https://doi.org/10.1016/j.biomaterials.2016.03.046

18. Ivanova L., Nikolov R., Tsikalova P., Nikolova M. Experimental rheoencephalographic studies on the effect of the cinnarizin analogue As_2 on cerebral circulation. *Acta Physiol Pharmacol Bulg*. 1979;5(2): 47–52. PMID: 517141.

19. Asadi P., Zia Ziabari S. M., Majdi A., Vatanparast K., Naseri Alavi S. A. Cinnarizine/betahistine combination vs. the respective monotherapies in acute peripheral vertigo: a randomized tripleblind placebo-controlled trial. *European Journal of Clinical Pharmacology*. 2019; 75(11): 1513–1519. https://doi.org/10.1007/s00228-019-02741-x

20. Shakeel F., Kazi M., Alanazi F. K., Alam P. Solubility of cinnarizine in (transcutol + water) mixtures: determination, hansen solubility parameters, correlation, and thermodynamics. *Molecules*. 2021;26(22): 7052. https://doi.org/10.3390/molecules26227052

21. Raghuvanshi S., Pathak K. Recent advances in delivery systems and therapeutics of cinnarizine: a poorly water soluble drug with absorption window in stomach. *Journal of Drug Delivery*. 2014;2014: 479–246. https://doi.org/10.1155/2014/479246

22.Polkovnikova Yu. A., Chistyakova V. M. Physicochemical and biopharmaceutical studies of solid dispersions of cinnarizine *Pharmaceutical Chemistry Journal*. 2023;57(3): 424–429. https://doi.org/10.1007/s11094-023-02900-6

23. Shahba A. A., Ahmed A. R., Alanazi F. K., Mohsin K., Abdel-Rahman S. I. Multi-layer self-nanoemulsifying pellets: an innovative drug Ddelivery system for the poorly water-soluble drug cinnarizine. *AAPS PharmSciTech*. 2018;19(5): 2087–2102. https://doi.org/10.1208/s12249-018-0990-7

24. Shahba A. A., Ahmed A. R., Mohsin K., Abdel-Rahman S. I., Alanazi F. K. Solidification of cinnarizine self-nanoemulsifying drug delivery systems by fluid bed coating: optimization of the process and formulation variables. *Die Pharmazie*. 2017;72(3): 143–151. https://doi.org/10.31083/ph.2017.6089

25. Sassene P. J., Mosgaard M. D., Löbmann K., ... Müllertz A. Elucidating the molecular interactions occurring during drug precipitation of weak bases from lipid-based formulations: a case study with cinnarizine and a long chain self-nanoemulsifying drug deliverys. *Molecular Pharmaceutics*. 2015;12(11): 4067–4076. https://doi.org/10.1021/acs.molpharmaceut.5b00498

26. Khan J., Rades T., Boyd B. J. Lipid-based formulations can enable the model poorly water-soluble weakly basic drug cinnarizine to precipitate in an amorphous-salt form during in vitro digestion. *Molecular Pharmaceutics*. 2016;13(11): 3783–3793. https://doi.org/10.1021/acs.molpharmaceut.6b00594

27. Buzlama A. V., Nikolaevskiy V. A., Chernov Yu. N., Slivkin A. I. *Preclinical studies of medicinal substances*. Moscow: GEOTAR-Media Publ.; 2017. 383 p. (In Russ.)

28. Andreev V. A., Andreeva E. Yu., Erdniev L. P., ... Apchel V. I. Using the Paramecium caudatum test object to determine the acute toxicity of physiologically active substances. *Bulletin of the Russian Military Medical Academy*. 2019;21(2): 110–113. (In Russ.). https://doi.org/10.17816/brmma25929

29. Rao J. V., Gunda V. G., Srikanth K., Arepalli S. K. Acute toxicity bioassay using Paramecium caudatum, a key member to study the effects of monocrotophos on swimming behaviour, morphology and reproduction. *Toxicological & Environmental Chemistry*. 2007;89(2): 307–317. https://doi.org/10.1080/02772240601010071

30. Polkovnikova Yu. A., Lenshin A. S., Kuznetsov A. Yu., Frolova V. E., Domashevskaya E. P. Sorption and toxicological properties of porous silicon nanoparticles with precipitated cinnarizine. *Sorbtsionnye i khromatograficheskie protsessy*. 2025;25(2): 211–222. (In Russ.). https://doi.org/10.17308/sorpchrom.2025.25/12960

31. Lenshin A. S., Kashkarov V. M., Seredin P. V., ... Domashevskaya E. P. Optical characteristics of porous silicon structures. *Technical Physics*. 2014;59(2): 224–229. https://doi.org/10.1134/s1063784214020145

32. Len'shin A. S., Kashkarov V. M., Goloshchapov ... Domashevskaya E. P. Composition and reactivity of porous silicon nanopowders. *Inorganic Materials*. 2012;48(10): 965–970. https://doi.org/10.1134/s0020168512100032

33. Polkovnikova Y. A., Lenshin A. S., Seredin P. V., Minakov D. A. Porous silicon nanoparticles containing neurotropic drugs. *Inorganic Materials*. 2017;53(5): 477–483. https://doi.org/10.1134/s0020168517050156

34. Spectral Database for Organic Compounds, SDBS. URL: https://sdbs.db.aist.go.jp/

35. Lipinski C. Lombardo A. F., Dominy B. W., Feeney P. J. Experimental and computational approaches to estimate solubility and permeability in drug discovery and development settings *Advanced Drug Delivery Reviews*. 1997;23(1–3): 3–25. https://doi.org/10.1016/s0169-409x(00)00129-0

36. Shabunin S. V., Buzlama V. S., Ermakova T. I., ... Maksimova L. N. Screening of biostimulating and biocidal substances (adaptogens, bactericides and other drugs). Moscow – Voronezh. In: *All-Russian Research Veterinary Institute of Pathology, Pharmacology and Therapy*. 2006. 51 p. (In Russ.)

37. Lenshin A. S., Peshkov Ya. A., Chernousova O. V., ... Agapov B. L. Effect of etching mode on the porosity of layers and photoluminescence in multilayer porous silicon. *Opticheskii zhurnal*. 2024;91(11):100-106. (In Russ.). https://doi.org/10.1364/jot.91.000771

38. Lenshin A. S., Polkovnikova Y. A., Seredin P. V. Study of the deposition process of vinpocetine on the surface of porous silicon. *Results in Physics*. 2016;6: 337–338. https://doi.org/10.1016/j.rinp.2016.06.008

39. Sassene P. J., Knopp M. M., Hesselkilde J. Z., Koradia V., Larsen A., Rades T. Precipitation of a poorly soluble model drug during *in vitro* lipolysis: characterization and dissolution of the precipitate. *Journal of Pharmaceutical Sciences*. 2010;99(12): 4982–4991. https://doi.org/10.1002/jps.22226

40. Uhanov Ju. I. *Optical properties of semiconductors*. Moscow: Nauka publ.; 1977. 366 p. (in Russ.)

Information about the authors

Evelina P. Domashevskaya, Dr. Sci. (Phys.–Math.), Full Professor, Department of Solid State Physics and Nanostructures, Voronezh State University (Voronezh, Russian Federation).

https://orcid.org/0000-0002-6354-4799

ftt@phys.vsu.ru

Aleksandr S. Lenshin, Dr. Sci. (Phys.–Math.), Leading Researcher, Department of Solid State Physics and Nanostructures, Voronezh State University (Voronezh, Russian Federation).

https://orcid.org/0000-0002-1939-253X

lenshinas@mail.ru

Yulia A. Polkovnikova, Dr. Sci. (Pharmacy), Associate Professor, Associate Professor of the Department of Pharmaceutical Technology and Pharmaceutical Chemistry, Faculty of Pharmacy, Voronezh State University (Voronezh, Russian Federation).

https://orcid.org/0000-0003-0123-9526

juli-polk@mail.ru

Vera E. Frolova, Cand. Sci. (Phys.–Math.), Associate Professor, Department of Solid State Physics and Nanostructures, Voronezh State University (Voronezh, Russian Federation).

https://orcid.org//0009-0000-2880-8958

ternovaya@phys.vsu.ru

Olga V. Chernousova, Cand. Sci. (Chem.), Lecturer, Voronezh State University of Engineering Technologies (Voronezh, Russian Federation).

byolval@mail.ru

Igor E. Zanin, Cand. Sci. (Phys.-Math.), ass. Prof., Assistant Professor, General Physics Department, Voronezh State University (Voronezh, Russian Federation).

iezan@mail.ru

Received March 6, 2026; approved after reviewing March 16, 2026; accepted for publication April 15, 2026; published online September 25, 2026.